Mission Performance Analysis for Conceptual Design of An Aerial Firefighting Aircraft

Technical Research Paper
Presented to the Faculty of the
School of Engineering and Applied Science
University of Virginia

By

Yicong Fu

May 8th, 2022

On my honor as a University student, I have neither given nor received unauthorized aid on this assignment as defined by the Honor Guidelines for Thesis-Related Assignments.

Signed: Yicong Fu

Approved: ______________________ Date May 9, 2022
Dr. Jesse R. Quinlan, Lecturer, Department of Mechanical and Aerospace Engineering

Introduction

Alarmed by the 2019-2020 Australian bushfire that burned approximately 240000 km^2 (Read & Denniss, 2020) and the 2020 California wildfires that claimed 33 lives (CalFire 2020), people have raised their attention to this type of catastrophic natural disaster mainly attributed to global warming and regional drought. According to the National Interagency Fire Center (NIFC 2019), the cost of personnel and equipment for fire suppression summed up to over $1.9 billion annually in the past decade and over $2.3 billion annually in the past 5 years. A scientific estimation has shown a continuation of this trend in the upcoming years. Currently, in large or remote fire sites, a 3D response with aerial crews is often necessary for rapid and effective personnel delivery, progression monitoring, and retardant deployment.

Modern firefighting aircraft are mainly retrofitted commercial or military airframes, which poses design limitations. Firefighting aircraft can be categorized into three groups based on their specific capabilities (CalFire 2019). Tactical aircraft such as Beechcraft King Air 200 and AH-1 Firewatch “Cobra” (Fig. 1) from CalFire are not equipped with payload tanks but are rather used for providing coordination and information about the spreading tendency. Helicopters such as Eurocopter AS332L and Boeing 234 Chinook (Fig. 2) are frequently used to drop water or retardant but most of their capacities are limited to 1000-3000 gallons due to size limitations. Airtankers such as the Boeing 747, DC-10, Boeing 737, and Lockheed C-130 (Fig. 3, 4) are able to carry more than 4000 gallons of payload to combat large fires, but repurposing costs them significant operational and structural inefficiencies.

Fig. 1. Beechcraft King Air 200 (left) and AH-1 Firewatch "Cobra" (right).

Fig. 2. Eurocopter AS332L (left) and Boeing 234 Chinook (right).

Fig. 3. Boeing 747 (left) and DC-10 (right).

Fig. 4. Boeing 737 (left) and C-130 (right).

To satisfy this expected demand for airtankers in the near future, my group from the MAE 4650-4660 Aircraft Design course decided to take on the challenge from the AIAA 2021-2022 undergraduate design competition for "Responsive Aerial Fire Fighting Aircraft". AIAA officially stipulated design requirements and objectives in the Request for Proposal (RFP) as summarized in Table 1, from which my team narrowed our scope to large and very large airtankers (LA/VLAT) (AIAA 2021).

Table 1. AIAA 2021-2022 undergraduate design competition RFP requirements and objectives.

Item	**Requirement**	**Objective**
Entry into service	• 2030 • Engine available before 2028 • Engine specs documented	• N/A
Capacity	• 4000 gal • Multi-drop capable • >= 2000 gal per drop • Reload >= 500 gal/min • Retardant density >= 9 lbs/gal	• 8000 gal
Payload drop	• Drop speed <= 150 kts • Drop altitude <= 300 ft	• Drop speed <=125 kts
Full-payload radius	• 200 nmi	• 400 nmi
Ferry range	• 2000 nmi	• 3000 nmi
Dash speed	• 300 kts	• 400 kts
Balanced field length	• <= 8000 ft (5000 ft MSL, +35 °F)	• <= 5000 ft (5000 ft MSL, +35 °F)
Certifications	• VFR and IFR capable • Icing resilient • FAA 14 CFR Part 25	• Systems and avionics for autonomous operations

Note that a thorough report on the final design is presented for the MAE 4660 capstone as a team effort, while this thesis is dedicated to covering my contributions as the performance analysis and mission modeling engineer in the group. Additional discussion related to how my work on a systematic level influenced specific design features is included in the current thesis, too.

Method

Comparator aircraft:

To assist valid ideation and decision-making, we chose several currently operating airtankers and transporters as baseline aircraft for design reference (Table 2). These existing models proved very helpful for constructing the fundamental configuration by comparing their capabilities with our aspired airframe. Their advantages and drawbacks were also evaluated for the room for improvements and modifications.

1. DC-10:

   The firefighting model was first put into service in 2006 as a retrofitted aircraft. This very large airtanker is able to carry up to 12000 gallons of payload (CalFire 2019). It is commonly used in large wildfires including the incidents in 2019 Australia and 2020 California. However, critics of this plane claim that it is relatively incapable of agile maneuvers due to its large size and dated design. Its weight upon arrival at the fire site is significantly lower than the designed maximum gross takeoff weight due to reduced mission block fuel, which decreases the cost-effectiveness. FAA records also show that the DC-10 is under 14 CFR Part 137 for agricultural aircraft operations instead of Part 25 for transport category airplanes (10 Tanker Air Carrier, 2018).

2. Boeing 737:

   The firefighting model was first put into service in 2018, retrofitted from N617SW. It is known as a large airtanker because of its 4000-gallon capacity (The Boeing 737 Technical Site, 2021). The large commercial retention of this model makes them rather available for repurposing. Their size enables them to be operated from both large hubs and some regional airports. However, their benefits over others are very marginal, in that

a) the capacity is not much higher than a large helicopter, b) their turnover rate is slower than helicopters, and c) they are less effective than DC-10 in large fires.

3. C-130:

   The firefighting model entered service around 1970-1980 after the US Congress created the Modular Airborne Fire Fighting System (MAFFS). Retrofitted military C-130s are able to carry 3000 gallons of retardant after being equipped with the MAFFS, making them a member of the airtanker family (USDA Forest Service). The modularized payload system consisting of five tanks and a specially designed valve enable them for multiple drops. However, since these airplanes were designed decades ago for military missions, they are limited to low altitudes, slow speeds, and short ranges by the engine and airframe choices. Age-related safety concerns also exist as there had been at least two crashes of the C-130 airtankers in 2002 (NTSB, 2002) and 2020 (Associate Press, 2020).

4. Boeing 757 (Fig. 5):

   So far there is no firefighting model retrofitted from it, but efforts have been made to convert one by 2024 (Cuenca, 2022). The freighter version such as B757-200F is able to carry 72210 lbs of payload, which is corresponding to 7221 gallons of retardant based on our density assumption (Boeing, 2007). This aircraft also has a good retention amount, and it uses modern avionics for controls. However, drawbacks do include old design and retrofitting inefficiencies like the DC-10.

Fig. 5. Boeing 757-200F

Table 2. Comparator aircraft useful specs (rough quantities).

	DC-10	**B737**	**C-130**	**B757**
Capacity (lb)	12000	4000	3000	7221
Length (ft)	182	100	97	155
Wing area (ft^2)	3550	1350	1745	1994
Wing sweep (deg)	35	25	0	25
Wing AR	7.5	9.45	10	7.8
OEW (lb)	240000	90000	80000	115000
MTOW (lb)	430000	160000	160000	255000

Analytical software:

To conduct performance analysis and mission-level estimation, both commercial and professional software were used to obtain quantitative results. These tools were particularly useful for constraining the design to the RFP requirements and objectives. The results from each software were further analyzed in-depth to understand the implications and used to inform subsequent analyses and decision-making in other design tools.

1. XFLR5: This is an airfoil evaluation tool that uses Lifting Line Theory, Vortex Lattice Method, and 3D Panel Method (XFLR5, 2021). It was used in the early stage for airfoil down-selection.
2. FLOPS: As known as the “Flight Optimization System”, this NASA software is the main tool for quantitatively estimating the weight and size of the aircraft. It requires input about configurational data from the 3D modeling software (OpenVSP), operational data,

and mission design data to compute fuel consumptions, weights, and mission details specifically for the RFP stipulations using our designed airframe.

3. SolidWorks: Specifically, the static simulation and analysis module was used to run finite element analysis on the wing geometry to check for stress and deformation under critical loading conditions.
4. OpenVSP: This is the CAD software used to construct a preliminary solid model of the aircraft. It is specifically engineered to assist with parametric geometric changes. Its own aerodynamics analysis package, VSPaero, was also used to evaluate aerodynamic performances. (Note: this is an auxiliary tool outside my major contributions.)
5. FlightStream: This software was mainly used for aerodynamic analysis and stability testing for the major airframe components. (Note: this is an auxiliary tool outside my major contributions.)

Results

Mission profile:

As the first step of the design process, defining the mission profile is necessary for weight estimation and aircraft sizing. With the RFP in mind, I devised the mission schedules as shown in Fig. 6 in order to meet as many requirements and objectives as possible.

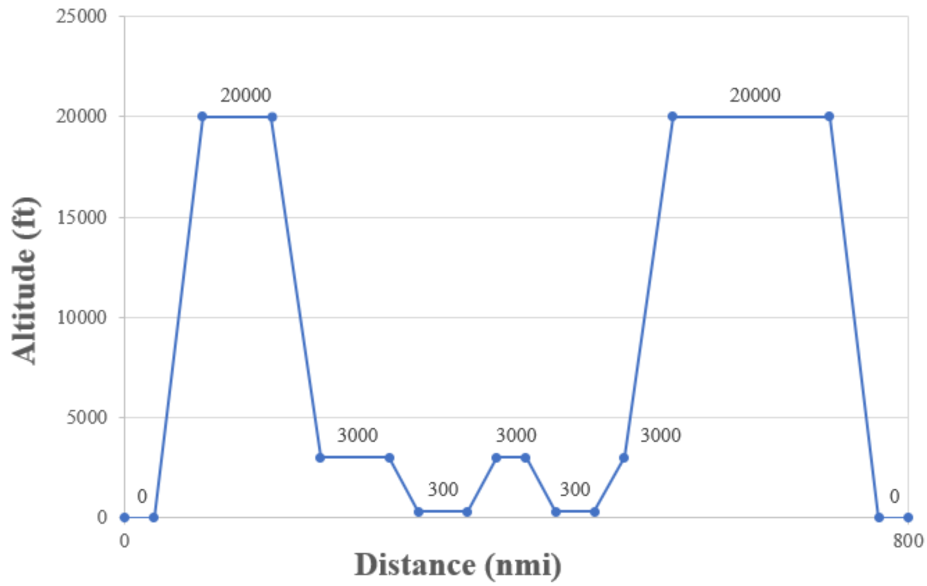

Fig. 6. Mission profile plotting segmental altitude as a function of flight distance.

Our aircraft is nominally designed to achieve two retardant drops within a mission radius of 400 nmi, or a total mission range of 800 nmi. The mission segments can be ordered chronologically as follows:

1. Mission starts with taxi-out and takeoff from the base airport.
2. The aircraft follows a standard constant-rate climb to the cruising altitude at 20000 ft heading towards the fire site.
3. The aircraft then enters a descent to 3000 ft level as it approaches the fire site and prepares for dropping.

4. Upon arrival at the fire site, the aircraft further descends to 300 ft to drop the first 4000 gallons of retardant.
5. The Aircraft then makes a quick dash back to 3000 ft towards the second dropping site.
6. Close to the second site, the aircraft makes another descent to the 300 ft level to drop the other 4000 gallons of payload.
7. The aircraft then makes another quick dash to 3000 ft to be clear from ground objects and terrains.
8. The aircraft proceeds with a return flight with the same climb and cruise schedules and finally descends back to the base airport for the next mission.

Weight and mission estimation:

To configure our preliminary aircraft from OpenVSP to operate the mission defined above, I relied on FLOPS to perform mission-level analysis on weight and fuel estimations. I transported the geometric information from OpenVSP into FLOPS as configurational input, which included basic data about the wing, tail, fuselage, fin, gear, and propulsion system. For the wing, major input data included the span, anhedral angle, area, aspect ratio, sweep angle, flap area ratio, number of sections, section span-wise locations, section chord lengths, sectional airfoil thickness-chord ratio, and span-wise engine positions. For the horizontal and vertical stabilizers, important inputs included their corresponding areas, sweep angles, aspect ratios, and taper ratios. Fuselage length, width, and height were also recorded to depict its size. Two fins were added to mimic the winglet design, and their area, aspect ratio, taper ratio, sweep angle, and thickness-chord ratio were inputted. A nominal landing gear specification for a similarly sized B757 was used as a placeholder. Finally, the propulsion system was defined by the number, thrust output, and weight of two RB211-535 turbofan engines. As operational input, I referred to

B737 and DC-10 to determine the appropriate number of flight crews onboard at three, consisting of one captain, one first officer, and one flight engineer. Other operational data including performance controls, factors, mission segment definition, ground operations, and field allowances were also determined with references to operating firefighting aircraft. For the mission design input, I followed the mission profile above to define the climb, cruise, and descent segments by their specific speed, altitude, and rate. Particularly for cruising conditions, three different schedules were set to cover the high-altitude-high-speed cruise at 20000 ft and 0.6-0.8 Mach, the mid-altitude-mid-speed preparation flight at 3000 ft and 0.45 Mach, and the low-and-slow drop period at 300 ft and 0.23 Mach. The schedules were set up as follows: standard taxi out and takeoff → standard climb to 20000 ft cruising altitude → cruise at 0.6-0.8 Mach for 350 nmi → descend to 3000 ft altitude → cruise at 0.45 Mach for 20 nmi → descend to 300 ft to drop 40000 lbs at 0.23 Mach → climb back to 3000 ft for 10 nmi for the second site → descend to 300 ft to drop 40000 lbs at 0.23 Mach → climb back to 20000 ft cruising altitude → return cruise at 0.6-0.8 Mach → final descent and approach → taxi in and end of mission.

1. Operating empty weight (OEW) (Fig. 7):

   Total structural weight was computed to be about 74500 lbs, including a 36400-lb wing, a 3950-lb horizontal tail, a 5000-lb vertical tail, a 14800-lb fuselage, and a 12200-lb landing gear system. Total propulsion weight was estimated to be around 17600 lbs, which included two RB211-535 turbofan engines that each added 8200 lbs of dry weight. Total system and equipment weight summed up to 14900 lbs to ensure that there are ample margins for surface control, APU, hydraulics, electrical wiring, avionics, equipment, and instruments. With crews, unusable fuel, engine oil, and cargo containers included, the total OEW was concluded at 133000 lbs. This takes up about 55% of the total takeoff gross weight. Double-checking the validity with reference aircraft showed that this value is indeed between the B737 (90000 lbs) and DC-10 (240000 lbs). Similarly sized B757 also confirms our estimation with its OEW around 115000 lbs.

MASS AND BALANCE SUMMARY	PERCENT WREF	POUNDS
WING	15.02	36424.
HORIZONTAL TAIL	1.63	3948.
VERTICAL TAIL	2.07	5014.
VERTICAL FIN	0.25	606.
CANARD	0.00	0.
FUSELAGE	6.09	14763.
LANDING GEAR	5.02	12169.
NACELLE (AIR INDUCTION)	0.66	1589.
STRUCTURE TOTAL	(30.72)	(74512.)
ENGINES	6.76	16404.
THRUST REVERSERS	0.00	0.
MISCELLANEOUS SYSTEMS	0.21	517.
FUEL SYSTEM-TANKS AND PLUMBING	0.28	668.
PROPULSION TOTAL	(7.25)	(17589.)
SURFACE CONTROLS	1.06	2560.
AUXILIARY POWER	0.20	490.
INSTRUMENTS	0.23	553.
HYDRAULICS	0.49	1179.
ELECTRICAL	0.69	1667.
AVIONICS	0.65	1570.
FURNISHINGS AND EQUIPMENT	2.32	5631.
AIR CONDITIONING	0.39	957.
ANTI-ICING	0.12	302.
SYSTEMS AND EQUIPMENT TOTAL	(6.15)	(14911.)
WEIGHT EMPTY MARGIN	4.12	10000.
WEIGHT EMPTY	48.25	117012.
CREW AND BAGGAGE-FLIGHT, 3	0.28	675.
-CABIN, 0	0.00	0.
UNUSABLE FUEL	0.16	399.
ENGINE OIL	0.07	168.
PASSENGER SERVICE	0.00	0.
CARGO CONTAINERS	6.13	14875.
OPERATING WEIGHT	54.89	133129.

Fig. 7. FLOPS weight estimation itemized breakdown showing OEW.

2. Takeoff gross weight (TOGW):

Also known as ramp gross weight or maximum takeoff weight (MTOW), this is the sum of the zero-fuel weight and the total mission fuel weight. FLOPS estimated the zero-fuel weight to be about 213000 lbs and the mission fuel to be 29400 lbs, which ultimately concluded to a TOGW of 243000 lbs, as shown in Fig. 8. A full-mission weight change profile is also plotted and shown in Fig. 9.

```
OPERATING WEIGHT                          54.89        133129.

     PASSENGERS,       0                   0.00             0.
     PASSENGER BAGGAGE                     0.00             0.
     CARGO                                32.98         80000.

ZERO FUEL WEIGHT                          87.88        213129.

     MISSION FUEL                         12.12         29406.

RAMP (GROSS) WEIGHT                      100.00        242535.
```

Fig. 8. FLOPS weight estimation showing mission fuel and TOGW.

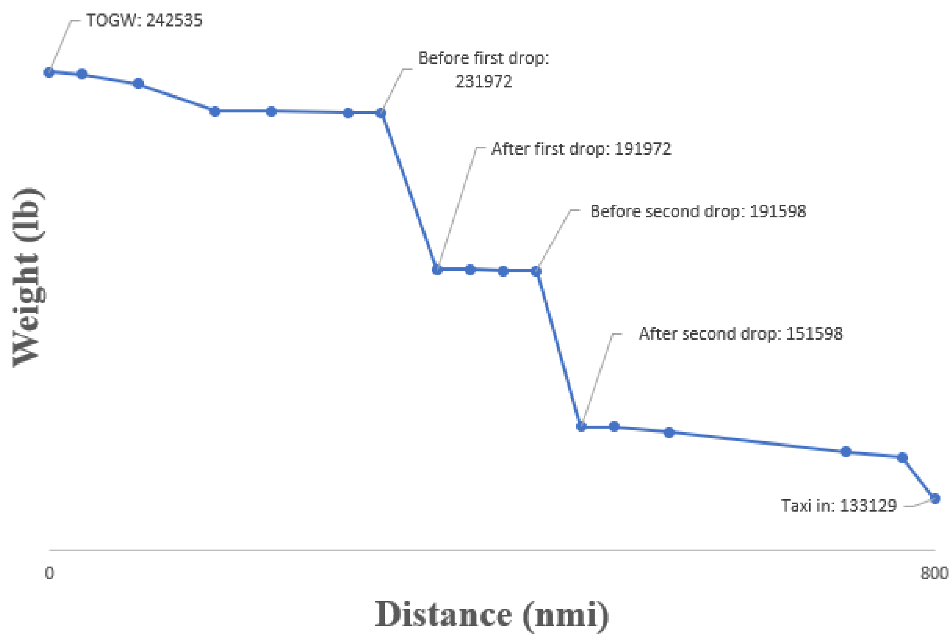

Fig. 9. Weight profile as a function of mission distance.

3. Segment fuel consumption:

   According to the mission summary (Fig. 10), I recorded the fuel consumption for each flight segment and computed their fuel weight fraction to identify the most energy-heavy flight condition for further optimization (Table 3). The vast majority of the fuel consumption occurs at climbs and 20000-ft cruises. This result indicates that further designing, testing, and analysis of the wing is necessary to ensure an optimized aerodynamic and aeroelastic performance. These optimizations will not only enhance fuel efficiency but also minimize the TOGW.

* * * M I S S I O N   S U M M A R Y * * *

	INITIAL	FUEL(LB)		TIME(MIN)		DIST (N MI)		MACH NUMBER		ALTITUDE(FT)	
SEGMENT	WT(LB)	SEGMT	TOTAL	SEGMT	TOTAL	SEGMT	TOTAL	START	END	START	END
TAXI OUT	242535.	434.	434.	10.0	10.0						
TAKE OFF	242101.	217.	650.	0.4	10.4				0.230		0.
CLIMB	241885.	2458.	3108.	5.7	16.1	29.1	29.1	0.230	0.600	0.	20000.
CRUISE	239427.	6874.	9982.	57.0	73.1	350.0	379.1	0.600	0.600	20000.	20000.
CRUISE	232552.	580.	10563.	4.1	77.2	20.0	399.1	0.450	0.450	3000.	3000.
RELEASE	231972.	0.	10563.	0.0	77.2	0.0	399.1	0.450	0.450	3000.	3000.
CRUISE	191972.	374.	10937.	3.9	81.1	10.0	409.1	0.230	0.230	300.	300.
RELEASE	191598.	0.	10937.	0.0	81.1	0.0	409.1	0.230	0.230	300.	300.
CLIMB	151598.	1457.	12394.	3.4	84.5	17.2	426.3	0.230	0.600	300.	20000.
CRUISE	150141.	4971.	17365.	44.5	129.0	273.4	699.7	0.600	0.600	20000.	20000.
DESCENT	145170.	1370.	18735.	29.4	158.5	100.3	800.0	0.600	0.300	20000.	0.
APPROACH	143799.	217.	18952.	1.0	159.5						
RESERVES	143583.	10454.	29406.								
TAXI IN		217.		5.0	164.5						
ZERO FUEL	133129.										

Fig. 10. FLOPS mission summary showing segmental fuel burn.

Table 3. FLOPS estimated segmental fuel weight fractions

Segment fuel weight fractions		
Segment	Weight (lb)	Fraction
Taxi-out	434	0.015
Takeoff	217	0.007
Climb	2458	0.084
Cruise 1 (20000 ft, 0.6-0.8 Mach)	6874	0.234
Cruise 2 (3000 ft, 0.45 Mach)	580	0.020
Release 1	0	0
Cruise 3 (300 ft, 0.23 Mach)	374	0.013
Release 2	0	0
Climb	1457	0.050
Cruise 1 (20000 ft, 0.6-0.8 Mach)	4971	0.169
Descent	1370	0.047
Approach	217	0.007
Reserves	10454	0.356
Taxi-in	217	0.007
Total	29406	1

Airfoil selection:

One of the most important features to optimize the wing is the airfoil which is essential for lift creation and drag reduction. Five airfoil types were initially considered, including under-cambered, flat-bottom, semi-symmetrical, and reflexed (Joyplanes, 2021). I evaluated their common applications in reality and their theoretical pros and cons and determined that the top two promising types were under-cambered and semi-symmetrical, as shown in Table 4.

Table 4. Comparison among five airfoil types.

Type	Image	Pros	Cons
Under-cambered	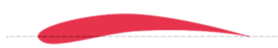	Good for slow flight. High life generation.	High drag from the wake.
Flat-bottom		Easily manufactured. Decent lift.	Relatively high drags.
Semi-symmetrical		Best lift-to-drag ratio.	More common for sports and aerobatic planes.
Symmetrical		Same lift generated in up and down directions.	Mainly used for precise aerobatic planes.
Reflexed		Auto stability correcting property.	Mainly used for flying wings and gliders.

To balance the benefits of using either airfoil type, I sought an airfoil on the transitional spectrum from under-cambered to semi-symmetrical shapes and conducted basic aerial performance simulations in XFLR5 to compare their lift and drag coefficients. Four airfoils were chosen: NACA 2412, NACA 4412, NACA 6412, and NACA 6409, ranking from the least under-cambered to the most under-cambered. Simulations were performed with Re = 3E+6 and swept across -20° to +20° for the angle of attack with an increment of 0.5°, assuming a 2D geometry without finite wing influences.

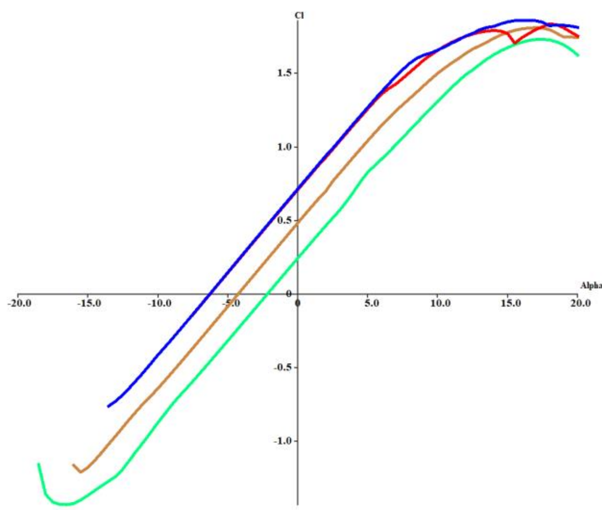

Fig. 11. Cl vs. alpha. NACA 6412 (red curve) shows the highest lift coefficient maximizing at around 16° of angle of attack. It also outputs a more reliable lift coefficient than NACA 6409 at high angles of attack.

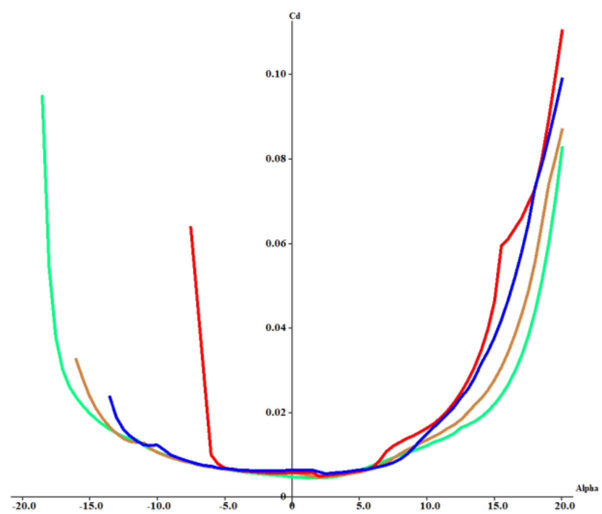

Fig. 12. Cd vs. alpha. All four airfoils seem to provide similar drag performance. Note that NACA 6409 airfoil has an earlier and drastic Cd increase as the angle of attack enters the negative domain around -5° to -8°, which corresponds to its tendency for flow separation at negative alpha.

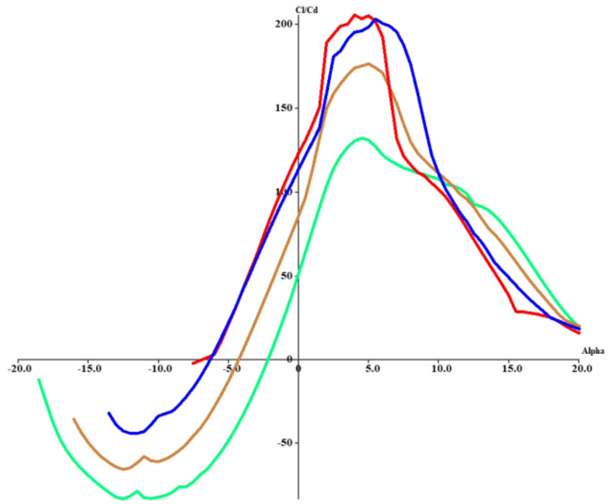

Fig. 13. Cl/Cd vs. alpha. NACA 6409 and NACA 6412 output the highest lift-to-drag ratio. This ratio optimizes at around 6 degrees for NACA 6412.

With the airfoil analysis shown above (Fig. 11, 12, 13), I determined that NACA 6412 provides the best overall aerodynamic performance by generating high lift with the relatively large camber and avoiding excessive drag build-up with the moderate under-camber. This same airfoil was used across the entire wing for two considerations: a) smooth and uniform surface shape in contact with the wind, and b) easier manufacturing.

Wing geometry optimization:

Zooming out to the macro scale, the shape and size of the wing planform were optimized in FLOPS for the purpose of minimizing fuel consumption and takeoff gross weight. I identified three major trade studies including wing area, wing sweep angle, and wing aspect ratio (AR).

1. Optimal wing area

   Our aspired payload capacity at 8000 gallons is right in the midpoint of the spectrum from B737 (4000 gallons) to DC-10 (12000 gallons). Assuming a linear relationship between aircraft size and cargo capacity, I estimated the wing area of our design to be between these two comparator models from 1350 ft^2 to 3550 ft^2 (RocketRoute, 2022 &

Modern Airliners, 2022). FLOPS was used to iterate through these values after which total mission fuel and takeoff gross weight were plotted as a function of the wing area, as shown in Fig. 14 & 15 below:

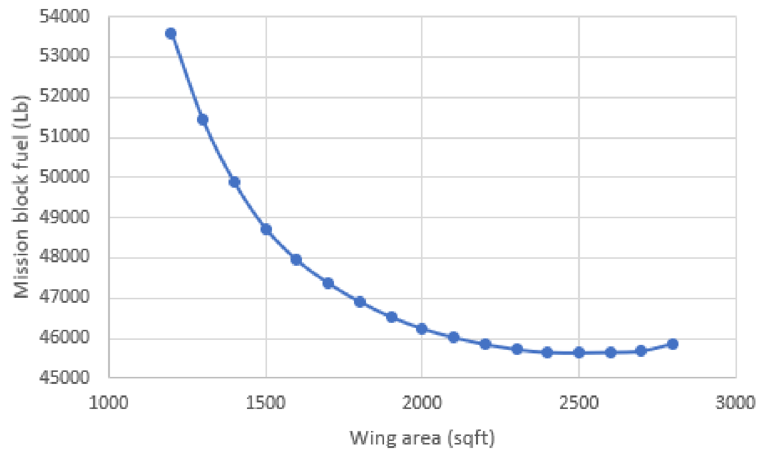

Fig. 14. Block fuel burn vs. wing area. Local minimum is around 2500 ft^2.

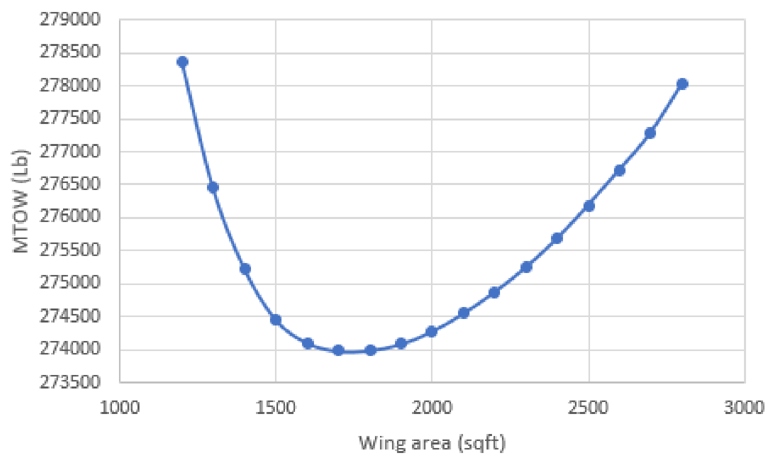

Fig. 15. Maximum takeoff weight vs. wing area. Local minimum is around 1750 ft^2.

Note that wing area is optimized at slightly different numbers for fuel consumptions and takeoff gross weight. To finalize the optimal wing area, these two criteria were equally weighted by 50% to evaluate the overall relationship, as shown in Fig. 16, where the local minimum falls around 2000 ft^2.

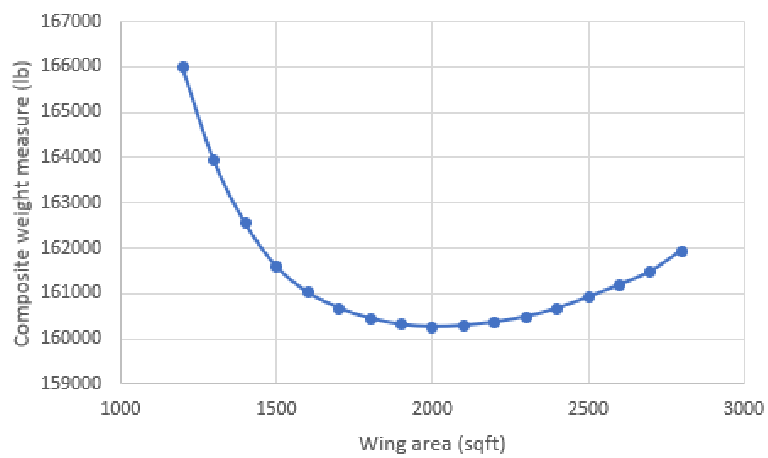

Fig. 16. Block fuel burn & maximum takeoff weight vs. wing area with equal weighting. The overall optimized wing area is around 2000 ft^2.

This optimized wing area is valid because it falls between the B737 and the DC-10 as expected. Further comparison with B757 which has almost the same cargo capacity and a wing area of 1994 ft^2 also confirms the analysis (Boeing 2007).

2. Optimal wing sweep angle

Wing sweep angles generally fall in three domains: negative (forward sweep), zero (no sweep), and positive (backward sweep), as exemplified in X-29, C-130, and Boeing 777 respectively (Table 5).

Table 5. Three types of wing sweep angles and their pros and cons.

Example aircraft	**Comments**
	• Experimental • Better stall maneuverability • Unstable to control
	• Operating • Relatively older design • Slower cruising speed • Structurally efficient • Earlier flow separation
	• Operating • Relatively new design • Transonic flight-capable • Better aerodynamic efficiency • Stricter margin for size and material

The same FLOPS analysis strategy was used to iterate through -4° to +52° for the wing sweep angle to cover as many designs as possible and necessary. Based on the results shown in Fig. 17, 18, & 19, I concluded that the optimal wing sweep angle was 36 degrees. This value makes sense as it is close to most of the latest commercial aircraft designs such as the Boeing 777 (+31.64°) (Modern Airliners, 2022), Boeing 787 (+32.2°) (Modern Airliners, 2022), and Airbus 350 (+31.9°) (Aviation Week, 2015). It is slightly higher than these operating models, but this can be explained by the following two reasons: a) FLOPS is an estimation tool that simulates under ideal conditions, so it is not capturing the exact fluid dynamics or aeroelastic performances, and b) the trend of having higher backward sweep somewhat agrees with the developmental history as new technology and material became available for aviation, as seen in Airbus 320 (+25°) (Modern Airliners, 2022) → Airbus 350 (+31.9°) or Boeing 737 (+25°) (Modern Airliners, 2022) → Boeing 787 (+32.2°). Meanwhile, we do need to acknowledge the possibility of this sweep angle being unrealistically high for the designed flight speed due to the analytical nature of FLOPS. FLOPS yields estimations based on theoretical equations and empirical data, which may not accurately reflect the weight constraints from aeroelastic, material, or maintenance aspects. Future analyses using high-fidelity simulations and experiments are highly recommended for corroborating the design.

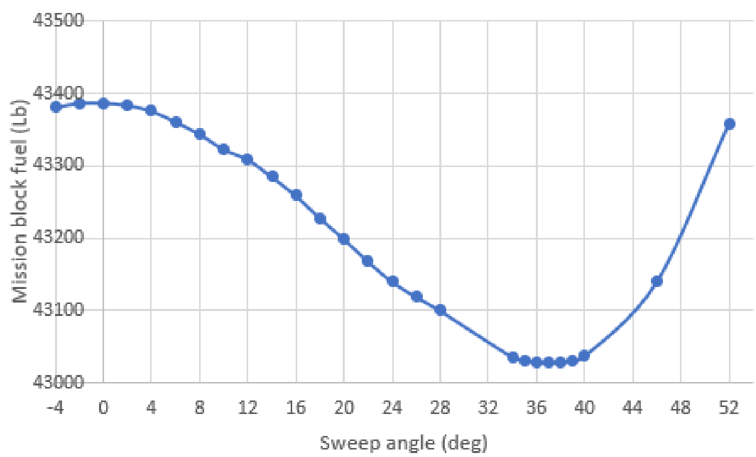

Fig. 17. Block fuel burn vs. Sweep angle.

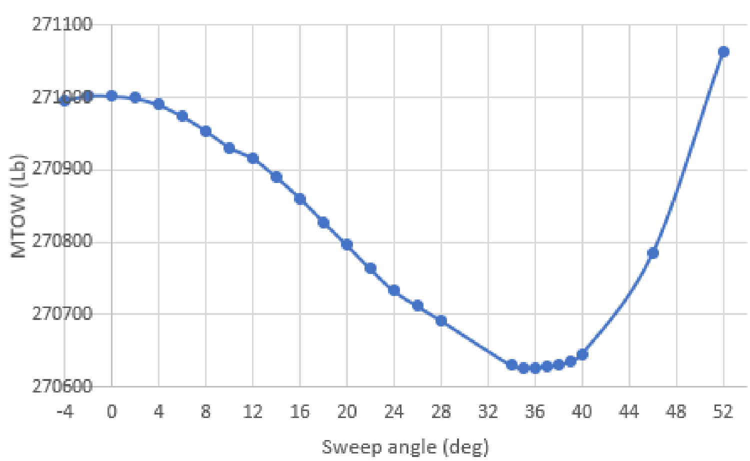

Fig. 18. Maximum takeoff weight vs. Sweep angle.

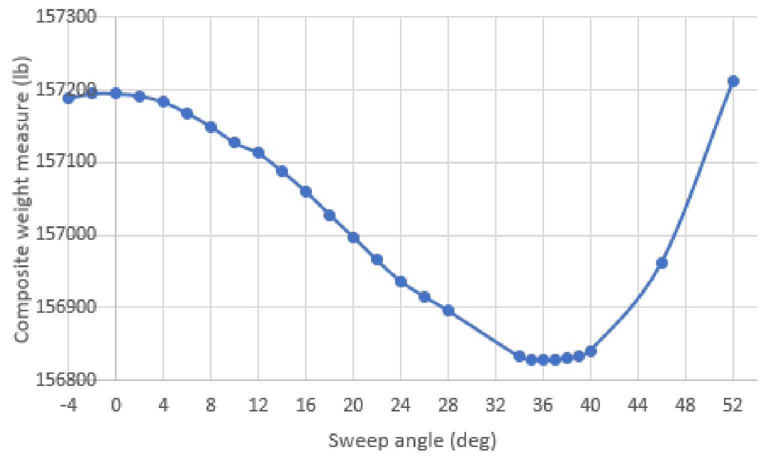

Fig. 19. Block fuel burn & Maximum takeoff weight vs. Sweep angle with equal weighting.

3. Optimal wing AR

Increasing the wing aspect ratio has been thought to be a way to increase efficiency because it shrinks down the induced drag term due to finite wings. Some efforts have been documented in the aviation industry and academia, such as the concept of Boeing SUGAR VOLT which essentially stretches a Boeing 737 wing from AR = 9 to AR = 18. Similar FLOPS analyses with AR from 5 to 20 were conducted and the results are shown below in Fig. 20, 21, & 22.

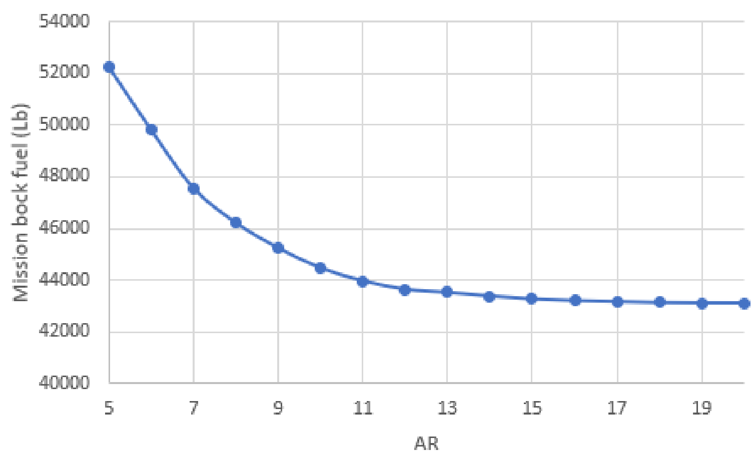

Fig. 20. Block fuel burn vs. AR.

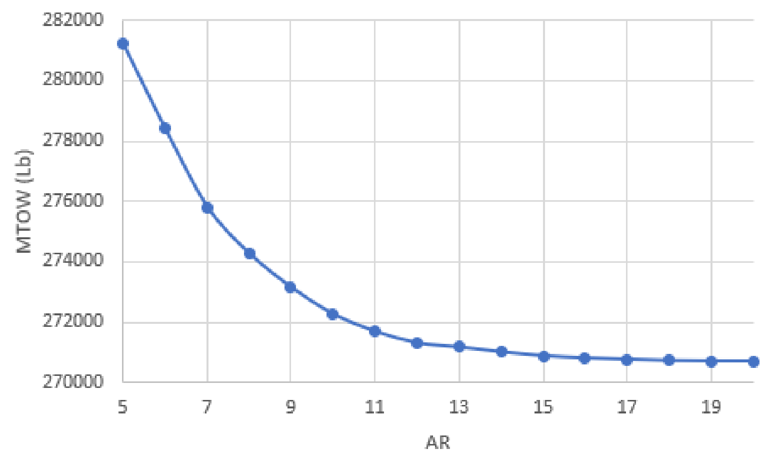

Fig. 21. Maximum takeoff weight vs. AR.

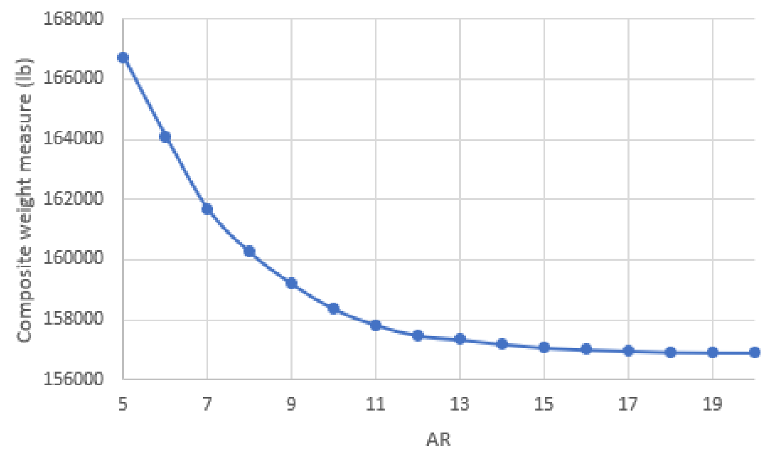

Fig. 22. Block fuel burn & Maximum takeoff weight vs. AR with equal weighting.

Initially, we were convinced that the wing aspect ratio optimizes after reaching about 13, hence the design of a long and slender wing planform. However, FLOPS sizing regressions are informed largely by existing, low-AR winged aircraft. Hence, the trust region for the FLOPS weight estimation regressions does not extend much higher than about AR 10-11, and any results above this AR likely do not account for significant sizing impacts due to dynamic aeroelastic sizing loads, which would serve to increase the wing weight - and decrease overall aircraft performance - relative to the FLOPS results shown here. An ultra-high aspect ratio can theoretically benefit the aerodynamic performance, but it could be limited by aeroelastic and material concerns. Therefore, further Finite Element Analysis (FEA) was conducted to test for stresses and deformations under extreme loading conditions.

Aeroelastic performance

To resolve the concern about our long and slender wing design from the ultra-high aspect ratio, SolidWorks Finite Element Analysis (FEA) was performed to verify structural rigidity and ground clearance under deformation. Four extreme loading cases were extracted from the V-n diagram made in MATLAB by my teammate Logan Honts (Fig. 23) and aspired mission schedules. In each static simulation, half of the wing was constrained as a cantilevered beam at the center cross-section. External loads considered include structural gravity (-z), distributive lift (+z), distributive fuel weight (-z), and engine weight (-z). Note that the wing is assumed to be a hollow aluminum structure with fuel compartments distributed inside. Material properties such as density were adapted based on the FLOPS-estimated weight and SolidWorks-calculated volume.

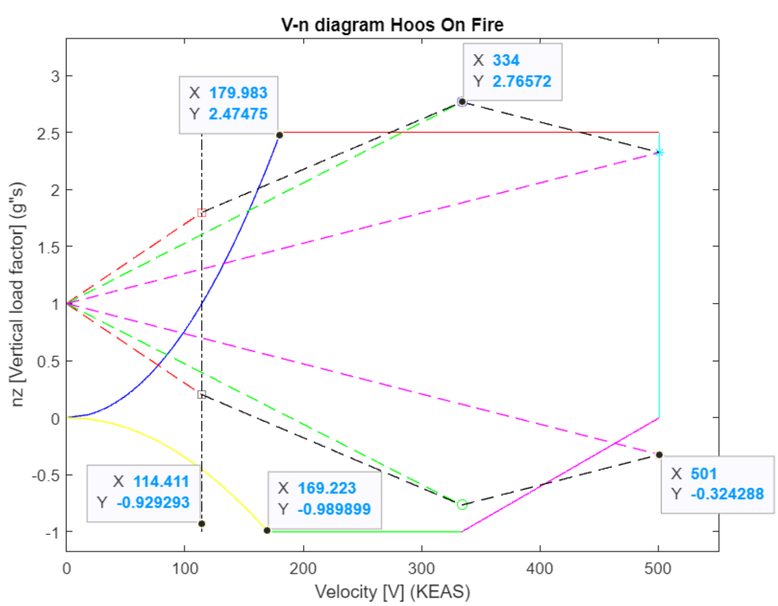

Fig. 23. V-n diagram showing max corner speed, sustained loadings, stall condition, and dive condition.

1. Takeoff with full payload

   External loads:

   a. Structural gravity = 18200 lbs (from FLOPS estimation)

      ($g = 9.81\ m/s^2$ | density = $0.0072645\ lb/in^3$ for hollow structure)

   b. Lift: TOGW/2 = 121267.5 lbs

   c. Fuel weight = Mission fuel/2 = 14703 lbs

   d. Engine weight = 8200 lbs

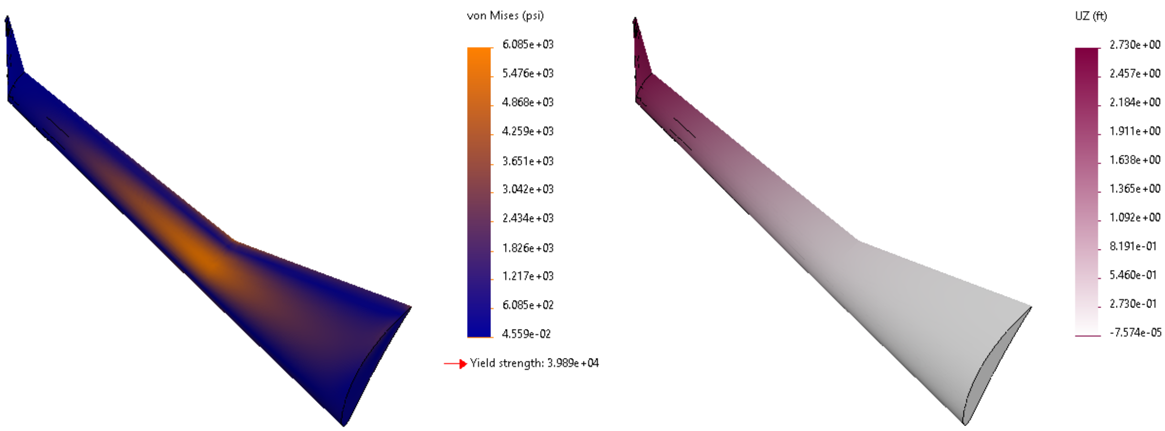

Fig. 24. Von Mises stress (left) & wing flex deformation (right) for full-payload takeoff.

   Results:

   a. Von Mises stress: 6.085E+3 psi < yield strength of 3.989E+4 psi

   b. Wingtip flex: 2.75 ft in +z direction.

2. Maximum critical load during flight

This is simulating a gust applying 2.8 times the regular maximum lift on the wing during a cruise.

External load:

a. Structural gravity = 18200 lbs (from FLOPS estimation)

(g = 9.81 m/s^2 | density = 0.0072645 lb/in^3 for hollow structure)

b. Lift: TOGW/2*2.8 = 339549 lbs

c. Fuel weight = 14700 lbs

d. Engine weight = 8200 lbs

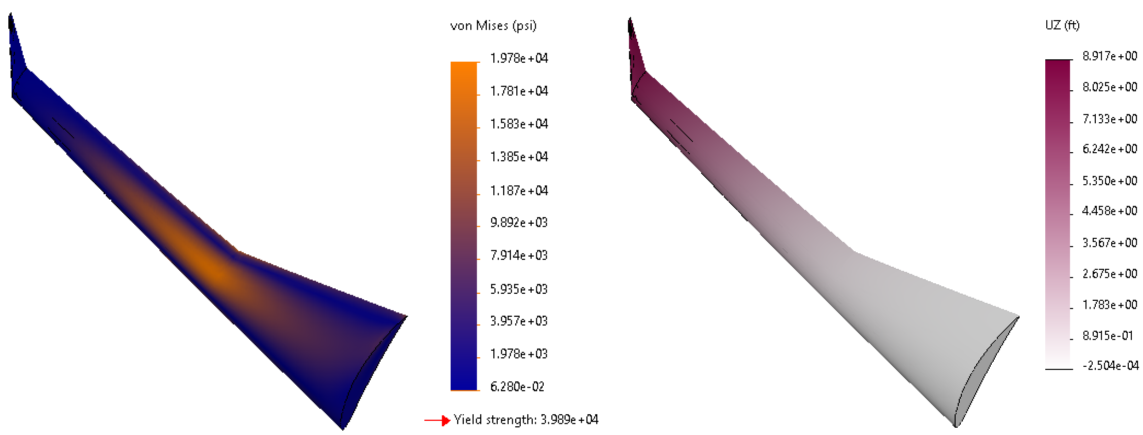

Fig. 25. Von Mises stress (left) & wing flex deformation (right) for maximum critical load.

Results:

a. Von Mises stress: 1.978E+4 psi < yield strength of 3.989E+4 psi

b. Wingtip flex: 8.917 ft in +z direction

3. 2g ramp bump

This is simulating a bump on the ground during taxi where a sudden change of acceleration adds twice the gravity on the structure.

External loads:

a. Structural gravity = 36400 lbs (from FLOPS estimation)

(g = 9.81*2 = 19.62 m/s^2 | density = 0.0072645 ln/in^3 for hollow structure)

b. Lift = 0 lbs

c. Fuel weight = 29406 lbs

d. Engine weight = 8200*2 = 16400 lbs

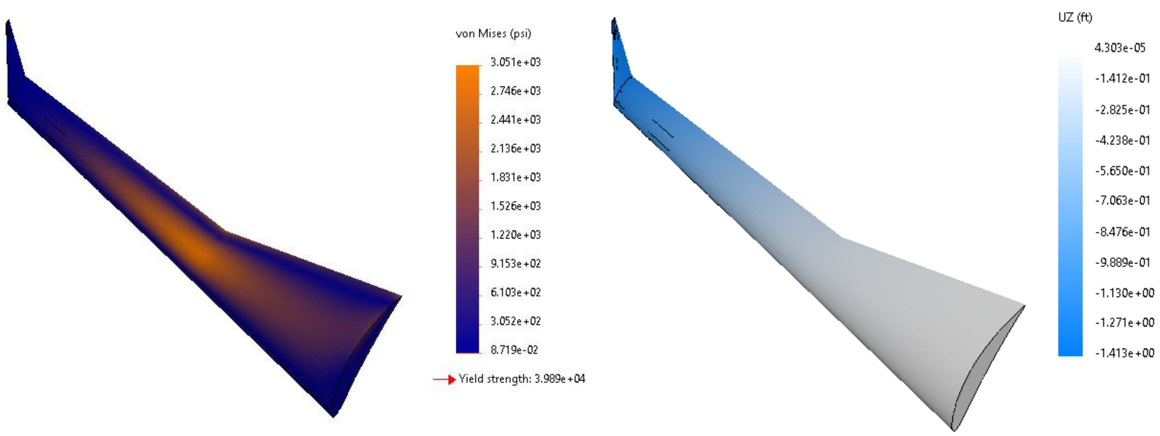

Fig. 26. Von Mises stress (left) & wing flex deformation (right) for 2g ramp bump.

Results:

a. Von Mises stress: 3.051E+3 psi < yield strength of 3.989E+4 psi

b. Wingtip flex: 1.413 ft in -z direction

4. -1g pull up load during flight

This is simulating special circumstances where the wing is loaded with lift forces in the negative direction during a pull-up maneuver.

External loads:

a. Structural gravity = 18200 lbs (from FLOPS estimation)

(g = 9.81 m/s^2 | density = 0.0072645 lb/in^3 for hollow structure)

b. Lift = -121267.5 lbs

c. Fuel weight = 14703 lbs

d. Engine weight = 8200 lbs

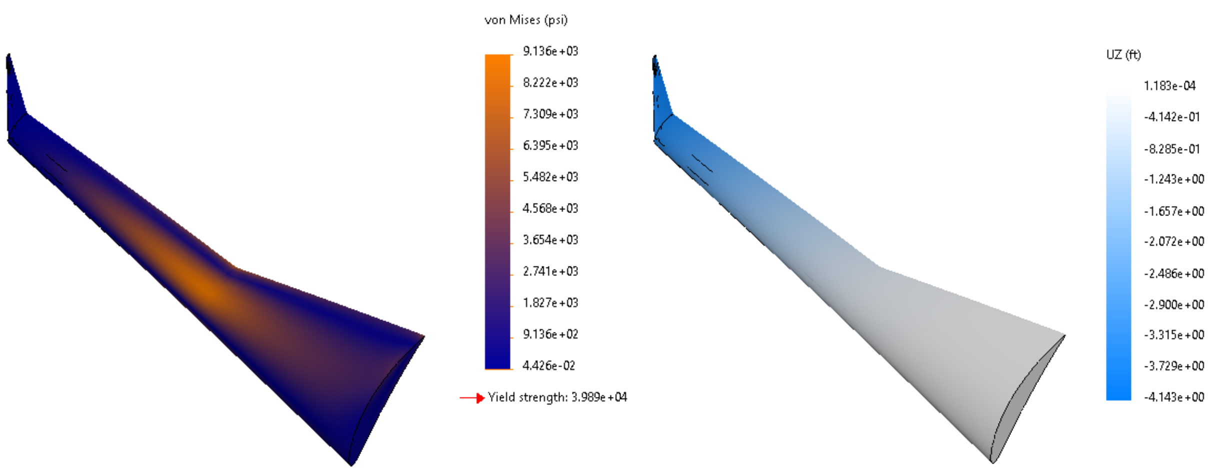

Fig. 27. Von Mises stress (left) & wing flex deformation (right) for -1g pull-up load.

Results:

a. Von Mises stress: 9.136E+3 psi < 3.989E+4 psi

b. Wingtip flex: 4.143 ft in -z direction

All of the FEA results indicate that the ultra-high aspect ratio wing is indeed operable in that: a) no stress concentration exceeds the yield strength of 6061 T6 Aluminum, b) wingtip deformations in the +z direction are well below the extreme case documented by Boeing with their B787 test up to 25 ft (Loh, 2022), and c) wingtip deformation in the -z direction guarantees ample ground clearance.

Note that these analyses were done under the assumption that the entire wing is made of 6061 T6 Aluminum, so values are calculated or compared with its particular material properties. Modern aircraft tend to use more composite materials such as polycarbonate, which usually yields even better mechanical properties than aluminum, so I concluded that this wing design is supported by the FEA results. However, other concerns about metal fatigue and simulation fidelity also exist. Since the aircraft will be expected to stay in service for a long time, loads under the yield strength can still cause catastrophic failure by propagating cracks to dangerous lengths. Theoretically, the larger the deformation is, the more likely it is for the wing material to fatigue and thus increasing maintenance costs. We, unfortunately, did not have enough time to perform a fatigue analysis, but do want to acknowledge the importance of further analysis. The basic static simulation in SolidWorks also has its own limitations because of the lack of wind flutters, gusts, and other dynamic perturbations. To help future developers improve the design, a lower aspect ratio wing (AR=9) was proposed and will be briefly discussed in the next section as an alternative option. Further enhancement of the geometry will incur changes in the OpenVSP CAD model, different configurational input in FLOPS, and modified FEA in SolidWorks or higher fidelity simulators, thus forming a feedback loop that continues to improve the mission-level performance and detailed design.

Final design:

The KeyShot rendered final design are shown in Fig. 28 & 29.

Fig. 28. Final design in ferry mission.

Fig. 29. Final design during retardant dump.

Discussion and future work

In this paper, I presented how my contributions as a mission-level performance analyst functioned as a spinal cord that connected different aspects of the firefighting aircraft design. Actor Network Theory would be a great conceptual framework to understand this workflow. Mission-level performance analysis is the “Obligatory Passage Point” (OPP) that forces all subordinate designs to converge on the RFP requirements and objectives. Through this focal point, each design process was evaluated for its validity and connections to other design features. Successful conclusions were documented and propagated forward, while failed attempts were revisited, revised, and returned to the feedback loop for modification. In this process, my work was crucial for its ability to tie all aspects together into a network and guarantee the design conformed to the AIAA RFP.

However, due to time and technical constraints, we acknowledge that the design has room to improve. Future work may tackle the following considerations.

1. Improve the FLOPS mission definition. The mission schedules defined in FLOPS currently only depict the most influential segments. Minor schedules such as loitering, short climbs, short descent, and fuel consumption during retardant dumps are not included. Adding these details will yield more accurate weight and fuel estimation.
2. Enlarge the airfoil pool. In our design cycle, only 5 airfoils were chosen for comparison, which was a bit limited. Those outside the NACA series such as Boeing airfoils are also worth trying because they have been tested by numerous professionals and real production applications. More thorough consideration of balancing the manufacturing difficulty and wingspan-wise airfoil change is also recommended.

3. Conduct higher fidelity simulations or wind tunnel experiments. Current aerodynamic analyses from VSPaero and FlightStream are limited because they don't reflect flow separation, transonic shock, or perturbations like gust and flutter. Solid mechanics analyses from SolidWorks also lack fatigue modeling. These are all possible scenarios that challenge the plane's safety, hence the importance to analyze stability and rigidity in these situations. Navier-Stokes solvers such as Autodesk CFD, wind tunnel tests, and computational mechanics are highly recommended in later design stages.
4. Try different geometries. As stated before, a low-AR wing was proposed to address the fluttering and fatigue concerns. Fundamental SolidWorks static simulation shows significant improvement in stress by a factor of 3.7 and in wingtip flex by a factor of 10. Further dynamic evaluation and mission-level performance analysis will help determine whether this is a better design.

Acknowledgment

The total aircraft design process was supported by team members of "Hoos on Fire" and advised by MAE 4650-4660 lecturer Dr. Jesse Quinlan. For a full description of the project, please refer to the corresponding AIAA submission.

References

AIAA (2021). Request for Proposal: Responsive Aerial Fire Fighting Aircraft. Retrieved from: https://www.aiaa.org/docs/default-source/uploadedfiles/education-and-careers/university-students/design-competitions/undergraduate-team-aircraft-design-competition/undergraduate-team-aircraft-design-2021-2022---aerial-fire-fighting-aircraft.pdf?sfvrsn=6d6f6ea5_0

Associate Press (2020). Three Americans killed as C-130 firefighting plane crashes in Australia. Retrieved from: https://www.latimes.com/world-nation/story/2020-01-22/australian-crews-search-for-firefight-plane-feared-crashed

Aviation Week (2015). Flying The A350: Airbus's Most Technologically Advanced Airliner. Retrieved from: https://aviationweek.com/air-transport/flying-a350-airbuss-most-technologically-advanced-airliner

Boeing (2007). 757-200F (Page 13). Retrieved from: boeing.com/resources/boeingdotcom/company/about_bca/startup/pdf/freighters/757f.pdf

CalFire (2019). Firefighting Aircraft Recognition Guide. Retrieved from: https://www.fire.ca.gov/media/4950/aviation-guide-2019-access.pdf

CalFire (2020). 2020 Incident Archive. Retrieved from: https://www.fire.ca.gov/incidents/2020/

Cuenca O. (2022). ST Engineering to convert Boeing 757 for use in aerial firefighting. Retrieved from: https://www.airmedandrescue.com/latest/news/st-engineering-convert-boeing-757-use-aerial-firefighting

Joyplanes (2021). Selection of Airfoil | Model Airplanes. Retrieved from: https://joyplanes.com/en/selection-of-airfoil-model-airplanes/

Loh C. (2022). How much can the Boeing 787's wings flex? Retrieved from: https://simpleflying.com/boeing-787-wings-flex/

Modern Airliners (2022). McDonnell Douglas DC-10, specs table. Retrieved from: https://modernairliners.com/mcdonnell-douglas-dc-10/

Modern Airliners (2022). Boeing 777 Specs, what makes this giant twin work? Retrieved from: https://modernairliners.com/boeing-777/boeing-777-specs/

Modern Airliners (2022). What are the Boeing 787 Dreamliner Specs? Retrieved from: https://modernairliners.com/boeing-787-dreamliner/boeing-787-dreamliner-specs/

Modern Airliners (2022). Airbus A320 Specs – what is behind one of the most popular short-haul airliners? Retrieved from: https://modernairliners.com/airbus-a320-introduction/airbus-a320-specs/

Modern Airliners (2022). Boeing 737 Specifications. Retrieved from: https://modernairliners.com/boeing-737/boeing-737-specifications/

NIFC (2019). Federal Firefighting Cost (Suppression Only). Retrieved from: https://www.nifc.gov/sites/default/files/document-media/SuppCosts.pdf

NTSB (2002). Accident report, NTSB Identification: LAX02GA201. Retrieved from: https://www.ntsb.gov/about/employment/_layouts/15/ntsb.aviation/brief2.aspx?ev_id=20020621X00954&ntsbno=LAX02GA201&akey=1

Read P. & Denniss R. (2020). With costs approaching $100 billion, the fires are Australis's costliest natural disaster. Retrieved from: https://theconversation.com/with-costs-approaching-100-billion-the-fires-are-australias-costliest-natural-disaster-129433#

RocketRoute (2022). Boeing 737-800, Dimensions. Retrieved from: https://www.rocketroute.com/aircraft/boeing-737-800#:~:text=Dimensions%3A,125.0m2%20(1344sq%20ft).

The Boeing 737 Technical Site (2021). 737-300 “Fireliner” Air Tanker. Retrieved from: http://www.b737.org.uk/fireliner.htm

USDA.Forest Service (U.S. Department of Agriculture Forest Service). Modular Airborne Fire Fighting Systems (MAFFS). Retrieved from: https://www.fs.usda.gov/managing-land/fire/planes/maffs

XFLR5 (2021). General Description. Retrieved from: http://www.xflr5.tech/xflr5.htm

10 Tanker Air Carrier (2018). Experience page. Retrieved from: https://web.archive.org/web/20180216120857/http://www.10tanker.com/experience.html